scientific reports

Check for updates

OPEN

# Scutellarin suppresses ovarian cancer progression by targeting METTL5

Ling Ding[1,7], Cenxin Luo[2,7], Nathaniel Weygant[3], Wutao Chen[4,5], Dan Ru[1], Yi Lai[6], You Wang[4,5]✉ & He Li[1]✉

**Scutellarin, a natural compound extracted from *Scutellaria barbata*, has demonstrated antitumor activity in various cancers. However, its role in ovarian cancer has not been fully explored. This study aims to evaluate the therapeutic potential and underlying mechanisms of Scutellarin in ovarian cancer. The effects of Scutellarin on cell proliferation and migration were assessed in ovarian cancer cell lines including SKOV3, A2780, OVCAR3, and OVCAR8. Patient-derived ovarian cancer organoids were used to further validate the in vitro findings. Calcein-AM and PI staining were used to analyze cell viability, and ATP assays were performed to assess organoid activity. Western blot was used to evaluate the regulation of METTL5 protein by Scutellarin. The gene and protein expression levels of METTL5 and their association with ovarian cancer prognosis were assessed using the databases The Human Protein Atlas (HPA), Gene Expression Profiling Interactive Analysis 2 (GEPIA2), TNMplot, KM-plotter and The Cancer Genome Atlas (TCGA). The functional role of METTL5 was assessed by transwell migration and colony formation assays, and its involvement in Scutellarin's mechanism of action was confirmed by rescue experiments using wound healing and transwell assays. Scutellarin significantly inhibited the proliferation and migration of ovarian cancer cells. In organoid models, Scutellarin markedly reduced organoid growth, induced cell damage, and decreased ATP levels. Compared to normal ovarian tissue, ovarian cancer tissue exhibited elevated RNA and protein expression levels of METTL5. High METTL5 expression was associated with poorer prognosis in ovarian cancer patients and promoted the migration and clonogenicity of ovarian cancer cells. Scutellarin downregulated METTL5 expression, and rescue experiments demonstrated that Scutellarin inhibited ovarian cancer migration by targeting METTL5. Scutellarin demonstrates potent, broad-spectrum anti-tumor activity in ovarian cancer cell lines, potentially mediated through targeting METTL5. These findings suggest a novel and promising therapeutic strategy for ovarian cancer treatment.**

**Keywords** Scutellarin, METTL5, Ovarian cancer, Patient-derived organoids, Anti-cancer therapy

Ovarian cancer, often diagnosed at an advanced stage due to its asymptomatic nature and anatomical location, exhibits substantial heterogeneity. Epithelial tumors are the most common type, further categorized into high-grade and low-grade serous carcinomas, endometrioid carcinoma, clear cell carcinoma, and mucinous carcinoma, with high-grade serous carcinoma being the most prevalent[1]. While surgery and chemotherapy are standard treatments, drug resistance, recurrence, and metastasis remain major obstacles. Thus, there is an urgent need for novel therapeutic strategies and further elucidation of the molecular mechanisms driving ovarian cancer progression.

Scutellarin, a flavonoid compound primarily derived from the extract of Erigeron breviscapus, is known for its anti-inflammatory and antioxidant properties. It exerts neuroprotective effects in ischemic brain injury by inhibiting inflammation and is effective in cardiovascular protection[2]. Recent studies have further explored the anti-cancer potential of Scutellarin, demonstrating its ability to induce apoptosis, inhibit cell proliferation

[1]Traditional Chinese Medicine Department, Renji Hospital, School of Medicine, Shanghai Jiao Tong University, Shanghai 200127, China. [2]Shanghai University of Traditional Chinese Medicine, 1200 Cailun Road, Shanghai 201203, China. [3]Academy of Integrative Medicine, Fujian University of Traditional Chinese Medicine, Fuzhou 350122, China. [4]Department of Obstetrics and Gynecology, Renji Hospital, School of Medicine, Shanghai Jiao Tong University, 160 Pujian Road, Shanghai 200127, China. [5]Shanghai Key Laboratory of Gynecologic Oncology, Renji Hospital, School of Medicine, Shanghai Jiao Tong University, 160 Pujian Road, Shanghai 200127, China. [6]Department of Head and Neck Surgery, Renji Hospital, School of Medicine, Shanghai Jiao Tong University, Shanghai 200127, China. [7] Ling Ding and Cenxin Luo equally contributed to this work. ✉email: wanghh0163@163.com; lihe1972@hotmail.com

and migration, and enhance chemotherapy sensitivity. It has shown inhibitory effects against various cancers, including renal[3], lung[4], liver[5], and breast cancers[6]. Preliminary studies suggest that Scutellarin may overcome platinum resistance in ovarian cancer by sensitizing cells to cisplatin[7], yet its efficacy and molecular targets warrant further investigation.

The METTL protein family, a subfamily of seven β-strand methyltransferases, possesses the ability to methylate nucleic acids, proteins, and small molecules[8]. METTL5 (methyltransferase-like protein 5), a key member of this family, functions as an RNA methyltransferase primarily responsible for catalyzing the m6A modification of 18 S rRNA, a modification essential for efficient protein translation in eukaryotic cells. Emerging evidence has demonstrated the oncogenic roles of METTL5 in various malignancies, including lung, gastric, liver, pancreatic, and renal cancers. For example, METTL5 promotes hepatocellular carcinoma progression through glucose metabolism reprogramming[9], enhances breast cancer cell proliferation by facilitating translation initiation[10], and drives immune evasion in gastric cancer via its overexpression[11]. Despite its potential as a therapeutic target in multiple tumor types, the role of METTL5 in ovarian cancer remains largely unexplored.

In this study, we examined the effects of Scutellarin on ovarian cancer cell lines originating from various tissue types. Our results demonstrate that Scutellarin significantly inhibits both the proliferation and migration of multiple ovarian cancer cell lines. Additionally, Scutellarin showed promising therapeutic efficacy in patient-derived ovarian cancer organoids, where it suppressed tumor growth and induced cell damage. We found that METTL5 is expressed at higher levels in ovarian cancer and is associated with a worse clinical prognosis. Notably, Scutellarin was shown to specifically target METTL5, suggesting that this may represent a key mechanism through which Scutellarin exerts its anti-cancer effects in ovarian cancer.

## Materials and methods

### Cell culure and establishment of stable cell lines

Human ovarian cancer cell lines SKOV3, A2780, OVCAR8, and OVCAR3 were purchased from the Shanghai Chinese Academy of Sciences Cell Bank and cultured in DMEM medium supplemented with 10% fetal bovine serum (FBS) and 1% penicillin–streptomycin. Passaging and experimental procedures were carried out during the logarithmic growth phase. For transfection, the METTL5 overexpression plasmid provided by GeneChem (Shanghai, China) was used. The constructed plasmid was co-transfected with packaging plasmids into HEK293T cells. After 48–72 h of transfection, the viral supernatant was collected, filtered to remove cell debris, and concentrated. The collected viral supernatant was used to infect SKOV3 cells, with medium replacement 24 h post-infection. Puromycin was applied to select for infected cells, generating stable METTL5-overexpressing SKOV3 cell lines. The overexpression of METTL5 was confirmed through Western blot analysis.

### CCK8 assay

SKOV3, A2780, OVCAR8, and OVCAR3 cells were seeded in 96-well plates and cultured until they reached 50–70% confluence after attachment, different concentrations of Scutellarin (MUST Bio, China) were added. After 24 h of incubation, 10 μL of CCK-8 reagent (TargetMol, China) was added to each well, and the cells were incubated for an additional 2 h at 37 °C. The optical density (OD) at 450 nm was measured using an enzyme plate reader. The OD value directly reflected the proliferative activity of the cells. The cell viability was plotted against drug concentration, and the $IC_{50}$ values for each cell line were calculated.

### Colony formation assay

Cells were seeded into 24-well plates, with an appropriate number of cells added to each well to ensure that individual cells could form colonies. Different concentrations of Scutellarin (10, 25, and 50 μM) were added. The culture was continued for 10 to 14 days until significant colony formation was visible. At the end of the experiment, cells were fixed with 4% paraformaldehyde, followed by crystal violet staining. Excess stain was washed off with PBS. After the cells dried naturally, colony formation was photographed, and the number of colonies was counted.

### Wound healing assay

Cells were evenly seeded into 24-well plates. Once the cells reached 90% confluence, a vertical scratch was made using a 200 μL sterile pipette tip to create a wound. After scratching, the suspended cells were removed and different concentrations of Scutellarin (10, 25, and 50 μM) were added. Phase-contrast images were captured at 0 h and 24 h using an inverted microscope. For each group, the wound healing percentage was calculated by comparing the residual wound width at 24 h to the initial wound width at 0 h within the same cell line, ensuring normalization across groups. Quantification was performed using ImageJ, and results were averaged from three independent technical replicates.

### Transwell migration assay

Cell suspensions treated with Scutellarin, without FBS, were added to the upper chambers of 8 μM transwell inserts (approximately $2 \times 10^4$ cells were seeded in each chamber), and DMEM medium containing 10% FBS was added to the lower chambers to induce cell migration. After 24 h of incubation, the cells that migrated through the membrane were fixed with 4% paraformaldehyde, while cells that did not penetrate the membrane were removed by staining with 0.1% crystal violet. Finally, the number of cells that migrated through the membrane was photographed and counted under a microscope.

### Treatment of patient-derived ovarian cancer organoids

Ovarian cancer tissues were obtained from patients through surgery, immediately washed with DPBS, and dissected into small fragments suitable for digestion, allowing the formation of single-cell clusters. The organoids

were cultured and maintained using the commercial Ovarian Cancer Organoid Kit (K2168-OC, bioGenous, China). The complete organoid culture medium was prepared according to the manufacturer's standardized "Formulation 3" protocol, which involved mixing concentrated supplements (B, C, D, F, and G) with the basal medium, as described in the product manual. This ensures a highly reproducible culture system. Following stable passaging, the organoids were seeded into 96-well clear-bottom black plates for subsequent drug treatment and growth assessment. Once the organoids neared maturity, different concentrations of Scutellarin and control treatments were applied. The number of organoids was recorded, and images were captured from five randomly selected fields. To assess cell viability, Calcein-AM and PI were added for live and dead cell staining, and corresponding 10× green/red fluorescence images were captured. ATP assays (AiMingMED, China) were performed to evaluate organoid activity.

## Bioinformatics analysis

Gene expression data from tumor and normal ovarian tissue samples were obtained via the GEPIA2 platform, which integrates RNA-Seq data from TCGA and GTEx by tissue type. For the ovarian cancer analysis, expression of METTL5 was examined using data from the TCGA-OV cohort ($n = 426$) and matched normal ovarian tissues from GTEx ($n = 88$). The expression values were normalized as transcripts per million (TPM) and visualized using box plots in log2(TPM + 1) format. No exclusion criteria were applied during sample selection. For pan-cancer analysis, both GEPIA2 and TNMplot (http:www.tnmplot.com) were used. GEPIA2 includes 9736 tumor and 8587 normal samples from TCGA and GTEx, while TNMplot integrates data from GEO, GTEx, TCGA, and TARGET, covering 15,648 normal and 40,442 tumor samples. Both platforms provide normalized RNA-Seq expression data and employ standardized pipelines to ensure consistency and reproducibility[12]. Ovarian cancer and normal ovarian tissue samples were sourced from the Human Protein Atlas (HPA), with METTL5 protein expression assessed by immunohistochemistry using the HPA038223 antibody. Antibody staining intensity and quantity were provided by the HPA. Survival analysis was performed using Kaplan-Meier (KM) curves, generated through the KM-plotter tool (https://kmplot.com/analysis/)[13]. For the ovarian cancer cohort, the METTL5 probe set (221570_s_at) was selected, and the optimal cut-off was determined, KM curves were then constructed for OS, PFS, and PPS. Univariate and multivariate Cox proportional hazards regression analyses were performed using the TCGA OV dataset downloaded from the Xena platform (xenabrowser.net). After excluding normal samples and those lacking METTL5 expression data, $n = 1202$ ovarian cancer samples were included. Hazard ratios (HR), 95% confidence intervals (CI), and p-values were calculated for each variable. Differential expression analysis between METTL5-high and METTL5-low subgroups was performed using TCGA ovarian cancer transcriptomic data. Genes with a log2 fold change $\geq 0.585$ or $\leq -0.585$ were considered significantly differentially expressed. KEGG pathway enrichment analysis and GO enrichment analysis were performed for the differentially expressed genes, with an adjusted P value $< 0.1$.

## Western blot

SKOV3 and OVCAR8 cells were treated with Scutellarin (10, 25, and 50 μM) for 48 h, after which the cells were collected, and protein was extracted using RIPA lysis buffer. The protein concentration was measured, and equal amounts of protein samples were mixed with SDS-PAGE loading buffer, boiled to denature, and loaded onto the gel for electrophoresis. The proteins were then transferred to a PVDF membrane. After blocking with BSA at room temperature, the membrane was incubated overnight with METTL5 primary antibody (1:2000, Proteintech, 16791-1-AP) and β-actin antibody (1:10000, Proteintech, 66009-1-Ig). After 1 h of incubation with the secondary antibody, the membrane was developed using chemiluminescent reagent (ECL), and bands were captured and analyzed.

## Molecular docking

The amino acid sequence of human METTL5 was retrieved from UniProtKB (https://www.uniprot.org/uniprotkb), and its corresponding three-dimensional structure was obtained from the RCSB PDB database (https://www.rcsb.org/). The protein structure was further optimized using Discovery Studio 2019, including the removal of water molecules, addition of polar hydrogens, completion of missing side chains and residues, and assignment of appropriate charges. The molecular structure of Scutellarin was obtained from PubChem and subjected to energy minimization in Discovery Studio 2019. Both the receptor and ligand were converted to PDBQT format using AutoDockTools (v1.5.6), with Gasteiger charges assigned and ligand torsional flexibility enabled. The docking grid was centered at coordinates (−0.527, −0.578, −4.215), with dimensions of $126 \times 126 \times 126$ points and a spacing of 0.375 Å, encompassing the predicted binding pocket. AutoGrid was used to generate affinity, electrostatic, and desolvation maps, applying a distance-dependent dielectric constant (dielectric = −0.1465). Molecular docking was performed using AutoDock Vina 1.2.6 with the Lamarckian Genetic Algorithm (LGA), running a total of 50 independent simulations with default parameters. The conformation with the lowest binding energy and highest cluster consistency was selected for further analysis, and the docking results were visualized and analyzed using PyMOL 3.1 and Discovery Studio 2019.

## Data analysis

All experiments were conducted with at least three independent biological replicates, and the data are presented as the mean ± standard deviation (SD). Statistical significance was determined using Student's t-test or ANOVA as appropriate. GraphPad Prism was used for data analysis and graphical representation.

## Results

### Scutellarin inhibits proliferation and clonogenic ability of ovarian cancer cell lines

We investigated the effects of Scutellarin on several commonly used ovarian cancer cell lines, including SKOV3, A2780, OVCAR3, and OVCAR8. To assess the impact of Scutellarin on ovarian cancer cell proliferation, we performed CCK-8 assays on these four cell lines. The results indicated that Scutellarin inhibited cell proliferation in a dose-dependent manner in SKOV3, A2780, and OVCAR8 cell lines, with $IC_{50}$ values of 176.9 μM, 142.7 μM, and 173 μM, respectively (Fig. 1A). However, no significant effect on cell viability was observed in OVCAR3 cells (Fig. 1A).

Based on existing studies of Scutellarin in both tumor[3,14] and non-tumor cell lines[15], we selected concentrations of 10, 25, and 50 μM for further functional assays. Previous literature has demonstrated that Scutellarin exhibits significant biological activity in other cell types, such as bronchial epithelial cells, within the concentration range of 20–100 μM, without inducing cytotoxic effects. Notably, no significant cell death response was observed even at concentrations as high as 400 μM[15]. These findings align with our observations in ovarian cancer cell lines. We found that 25 μM of Scutellarin effectively reduced colony formation in all four cell lines. At 50 μM, Scutellarin resulted in a more than 50% reduction in colony count compared to the control group. Notably, colony formation was suppressed in all cell lines at concentrations well below their respective $IC_{50}$ values, suggesting that Scutellarin may exert anti-tumor effects through modulating cellular processes, rather than directly inducing cell death (Fig. 1B,C). These findings collectively demonstrate that Scutellarin

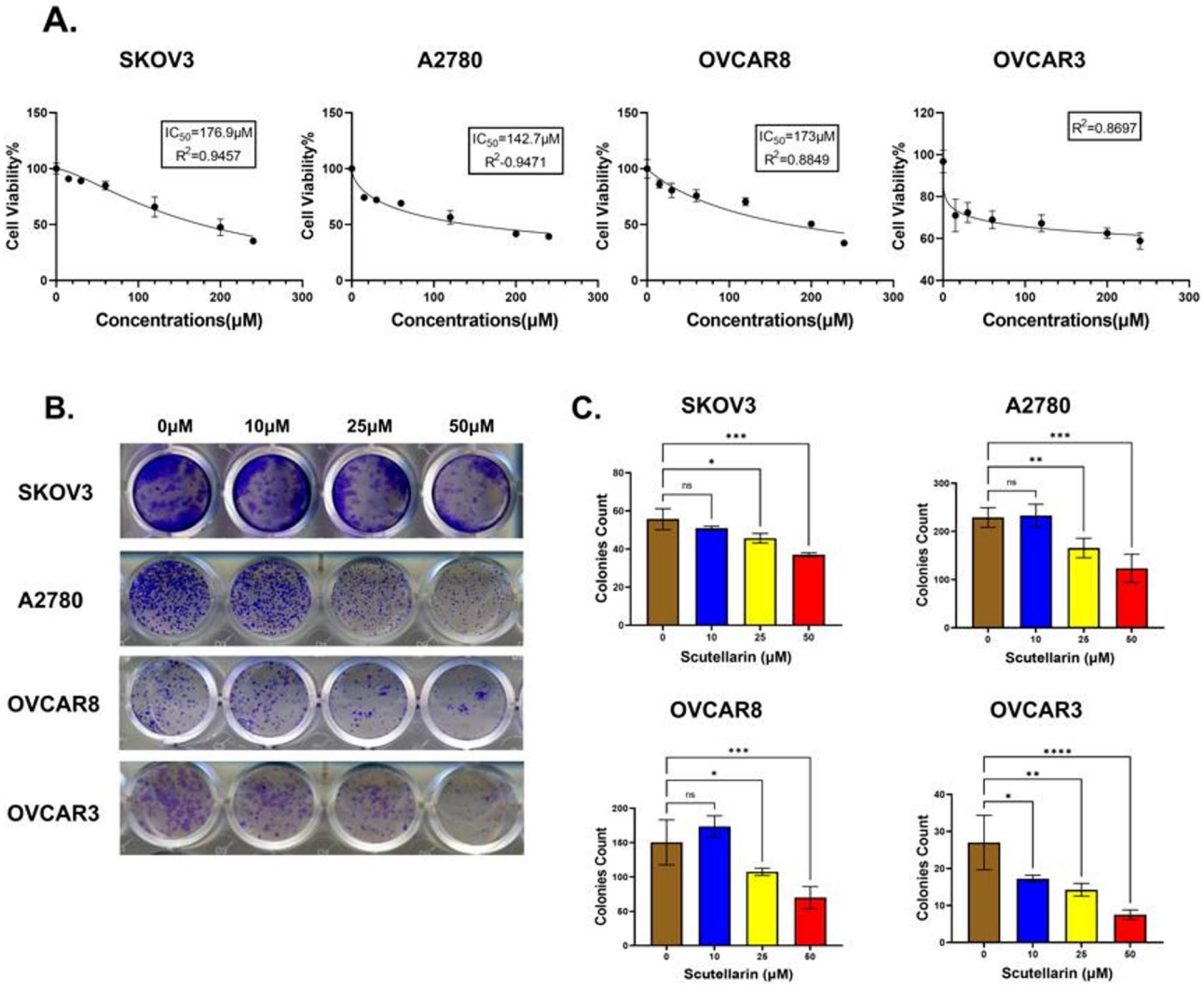


**Fig. 1**. Scutellarin inhibits the proliferation of SKOV3, A2780, OVCAR8, and OVCAR3 ovarian cancer cell lines. (**A**) Cell proliferation was assessed using the CCK8 assay, with Scutellarin concentrations ranging from 0 to 240 μM. The $IC_{50}$ values for inhibition are presented in the figure. (**B**) Representative images of colony formation assays following treatment with 0, 10, 25, and 50 μM Scutellarin, showing that Scutellarin significantly suppresses the clonogenic ability of cell lines. (**C**) Quantitative analysis of colony formation, with statistical significance indicated by $^{*}P<0.05$, $^{**}P<0.01$, $^{***}P<0.001$, $^{****}P<0.0001$.

effectively suppresses clonogenicity and cell proliferation in ovarian cancer cell lines from various histological subtypes, at non-toxic concentrations.

### Scutellarin impairs the migration ability of ovarian cancer cell lines

To further investigate the effects of Scutellarin on the migratory capacity of ovarian cancer cells, we treated SKOV3, A2780, OVCAR3, and OVCAR8 cell lines with Scutellarin at concentrations of 10, 25, and 50 μM, and evaluated wound healing at 24 and 48 h (Fig. 2A). In the highly migratory SKOV3 cells, treatment with 25 μM Scutellarin significantly inhibited migration at the 24 h time point (Fig. 2B). In the high-grade serous ovarian cancer cell lines OVCAR3 and OVCAR8, 50 μM resulted in a significant decrease in wound closure relative to controls (Fig. 2B). The scratch migration ability of A2780 was not affected by the drug treatment (Fig. 2B).

To further validate these findings, we performed transwell migration assays, which corroborated the results from the wound healing assays, as shown in the representative pictures (Fig. 3B). Scutellarin inhibited

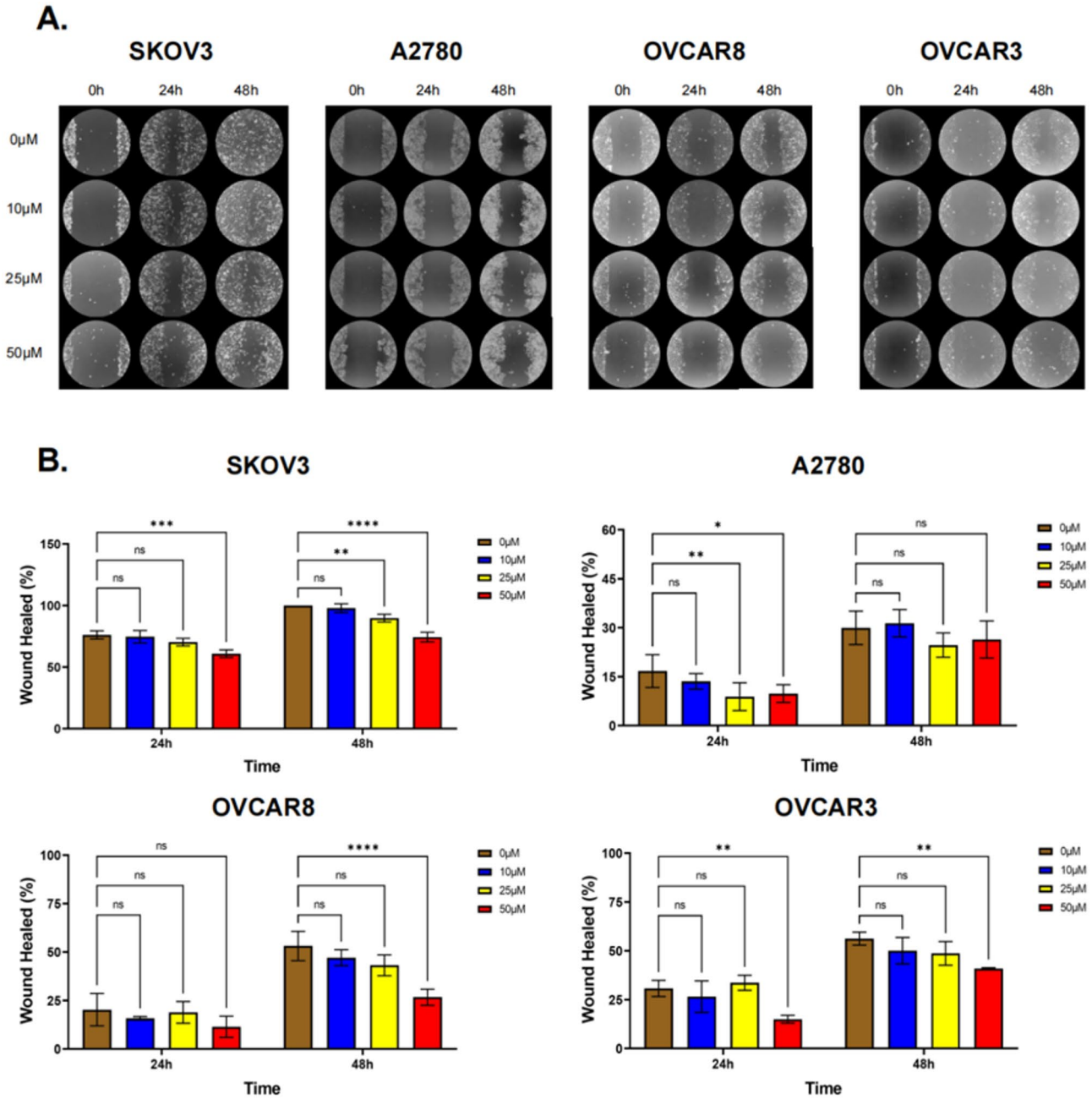


**Fig. 2**. Wound healing assay to examine the effect of Scutellarin on ovarian cancer cell lines. (**A**) Representative images of wound healing at 24 h and 48 h after Scutellarin treatment (0, 10, 25, 50 μM) in SKOV3, A2780, OVCAR8, and OVCAR3 cells. (**B**) Quantification of the wound closure percentage in the four cell lines. $^{*}P<0.05$, $^{**}P<0.01$, $^{***}P<0.001$, $^{****}P<0.0001$.

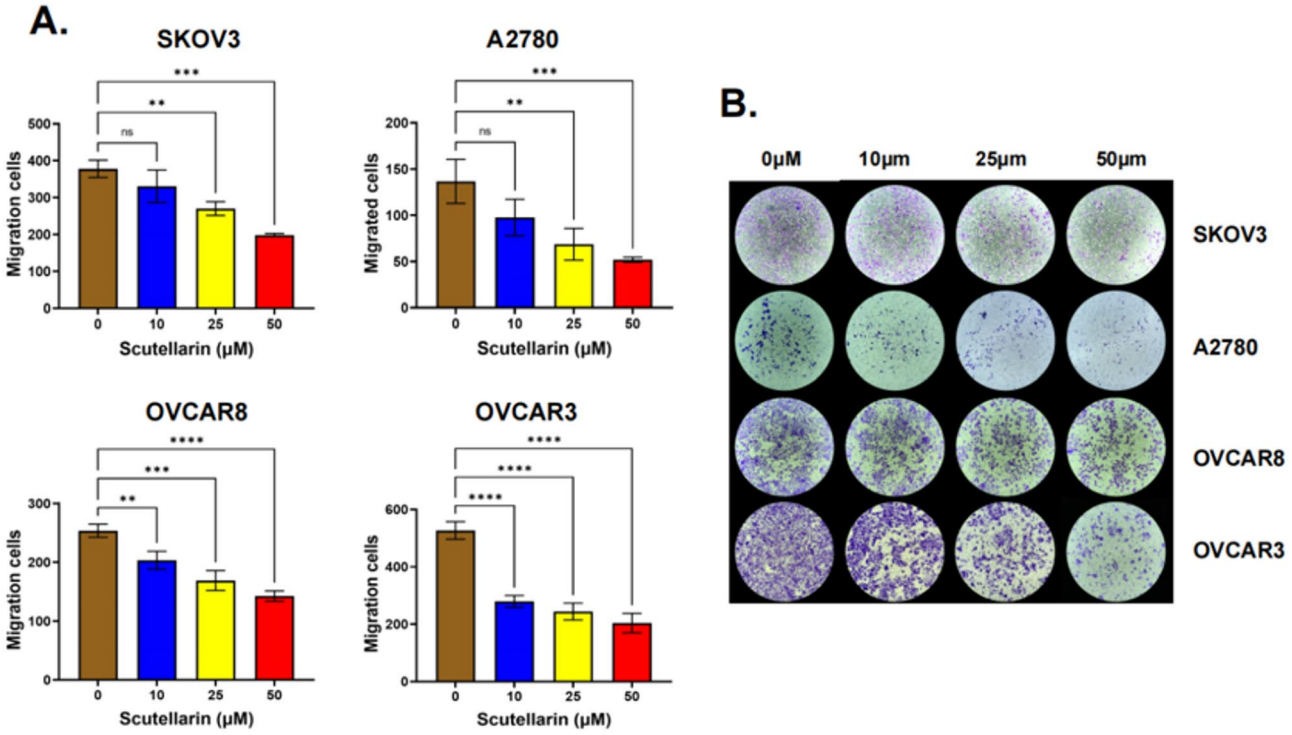


**Fig. 3**. The inhibitory effect of Scutellarin on the migration ability of ovarian cancer cell lines was determined by the transwell migration assay. (**A**) Quantification of transwell migration cells of SKOV3, A2780, OVCAR8, and OVCAR3 after 24 h treatment with 0, 10, 25, and 50 μM Scutellarin. (**B**) Representative images of transwell migration. $^{**}P<0.01$, $^{***}P<0.001$, $^{****}P<0.0001$.

cell migration in a dose-dependent manner across all four cell lines at the 24 h time point. Notably, a lower concentration of 10 μM Scutellarin demonstrated significant inhibitory effects on migration in both OVCAR3 and OVCAR8 cells. In the 50 μM concentration group, the number of migrated cells in both A2780 and OVCAR3 cell lines decreased by more than half (Fig. 3A). Collectively, these data suggest that Scutellarin impairs the migratory properties of ovarian cancer cells, thereby highlighting its potential as a therapeutic agent to inhibit the malignant progression of ovarian cancer.

## Scutellarin inhibits the growth and viability of ovarian cancer organoids

Organoids derived from various tumor types have become an essential tool in cancer research and drug testing due to their ability to preserve the molecular and histological features of the original tumors, thereby reflecting patient-specific tumor characteristics. Organoids are particularly valuable for studying the mechanisms of ovarian cancer initiation and progression, as well as for drug development and the design of personalized therapeutic strategies[16,17]. Ovarian cancer organoids are typically generated from primary tumor cells obtained from patient biopsies and can be efficiently expanded in vitro. In this study, we established ovarian cancer organoids from two distinct histological subtypes: endometrioid and high-grade serous ovarian cancer. The endometrioid organoids exhibited a compact, rounded morphology with a dense central structure, while high-grade serous ovarian cancer organoids displayed increased cellular cohesion and a more irregular shape, with reduced roundness, in line with previously reported characteristics in the literature[18].

We treated both types of organoids with Scutellarin and monitored changes in organoid number. Scutellarin significantly inhibited the size and quantity of both organoids (Fig. 4A,C). At the end of the experiment, marked morphological collapse was observed in both organoid types following drug treatment, with a more pronounced effect in organoid 1. At 10 μM, Scutellarin significantly reduced organoid size, while the 25 μM group showed noticeable morphological shrinkage and cellular breakdown. In organoid 2, membrane vesicle formation was observed, damaged cells detached from the lumen, and "apoptotic blebbing" accumulated around the organoid (Fig. 4A).

Further analysis using Calcein-AM and PI staining allowed for clearer visualization of live and dead cells within the organoids. After treatment, in addition to a reduction in organoid volume observed in brightfield images, organoid#1 showed pronounced surface membrane damage, whereas organoid#2 exhibited more widespread cellular breakdown originating from the inner core (Fig. 4B). ATP assays at the experimental endpoint further confirmed that Scutellarin significantly reduced organoid viability (Fig. 4C). These findings confirm that Scutellarin exerts potent therapeutic effects across ovarian cancer organoids derived from different histological subtypes, reinforcing its potential as an effective therapeutic candidate for ovarian cancer and supporting its clinical relevance, complementing the results from cell line-based results.

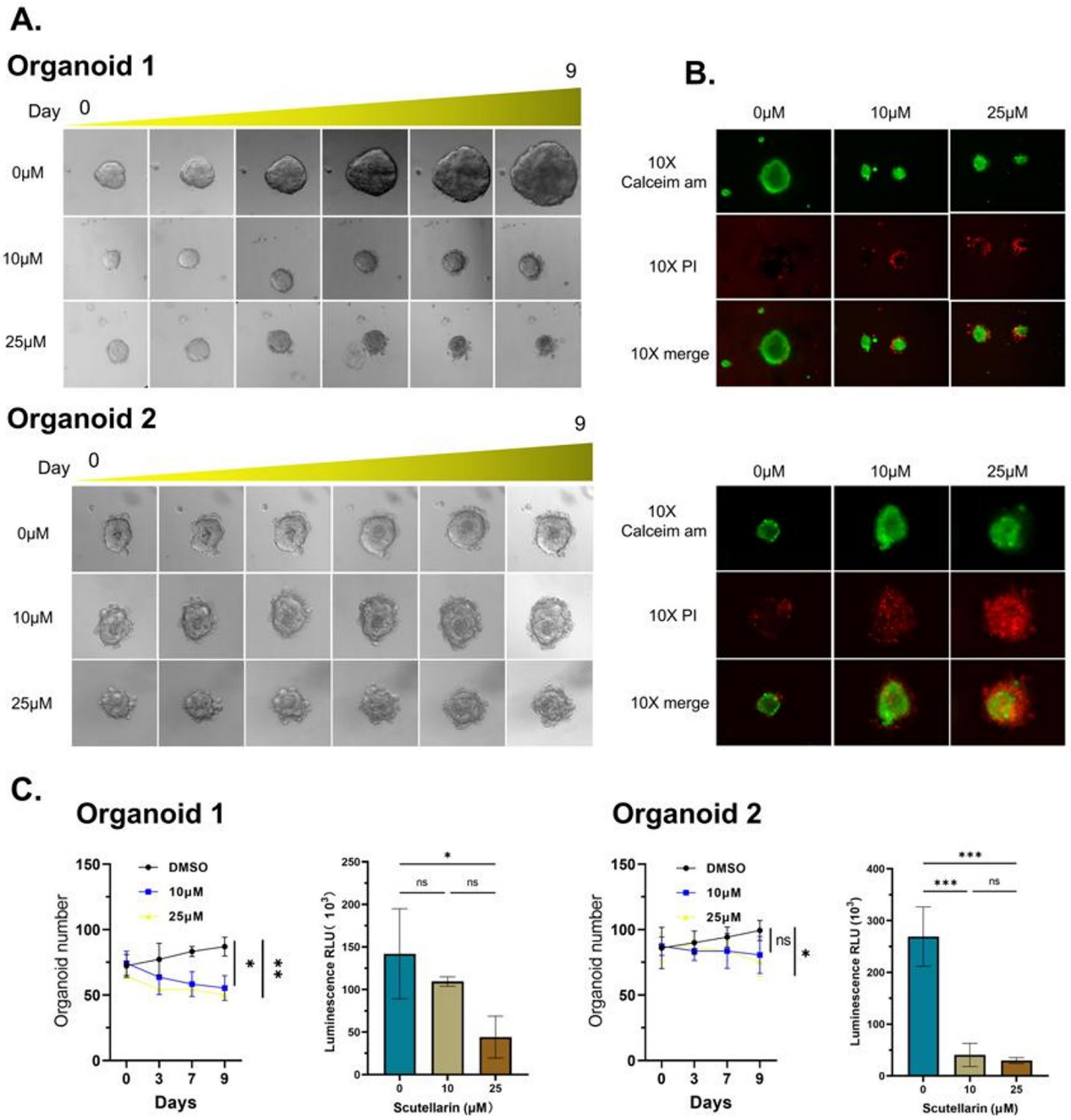


**Fig. 4**. Scutellarin inhibits the growth and viability of ovarian cancer organoids. (**A**) Scutellarin significantly inhibited the size and quantity of both organoids. (**B**) At the experimental endpoint, Calcein-AM (green) and PI staining (red) were used to label live and dead cells in organoids. Representative images at 10× magnification and the merged images are shown. (**C**) Quantification of organiod number and viability. $^{*}P < 0.05$, $^{***}P < 0.001$.

## Scutellarin targets METTL5 to inhibit ovarian cancer progression

Western blot analysis showed that treatment with Scutellarin (50 μM) markedly downregulated METTL5 expression in both SKOV3 and OVCAR8 cells. Densitometric quantification showed a 34% reduction in SKOV3 and a 65% reduction in OVCAR8 cells, providing quantitative support for the inhibitory effect of Scutellarin on METTL5 (Fig. 5B). To further investigate the role of METTL5 in ovarian cancer, we overexpressed METTL5 in the SKOV3 cells and confirmed a 74% increase in protein level via densitometric analysis (Fig. 5A). Functionally, METTL5 overexpression resulted in a significant increase in both colony formation and cell migration (Fig. 5C,D). Molecular docking studies revealed a strong binding interaction between Scutellarin and METTL5. Specifically, Scutellarin binds to the active pocket of METTL5, forming stable hydrogen bonds with key surface residues, with a binding energy of -6.76 kcal/mol (Fig. 5G). To determine whether METTL5 is involved in

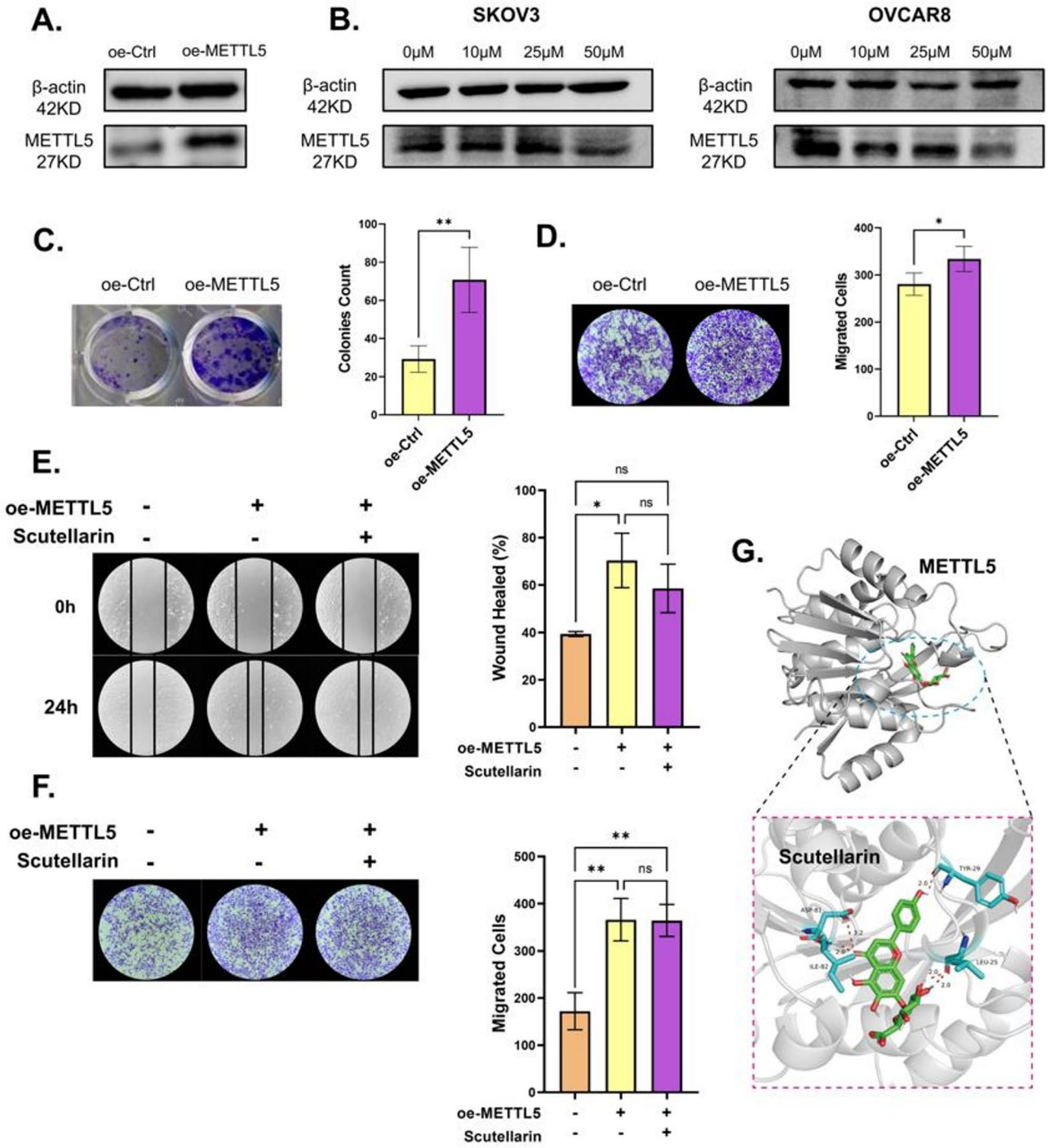


**Fig. 5**. METTL5 promotes ovarian cancer proliferation and migration, and Scutellarin exerts its effects by targeting METTL5. (**A**) Western blot validation of METTL5 overexpression efficiency in SKOV3 cells. (**B**) METTL5 expression in SKOV3 and OVCAR8 cell lines after treatment with Scutellarin at concentrations of 0, 10, 25, and 50 μM, with significant downregulation at 50 μM. (**C**) Colony formation assay comparing proliferation between oe-METTL5 and oe-Ctrl in SKOV3 cells, with quantitative analysis of colony numbers. (**D**) Transwell migration assay showing increased migration in oe-METTL5 SKOV3 cells compared to the control, with quantification of migrated cell numbers. (**E**) Wound healing assay demonstrating the impact of METTL5 overexpression and Scutellarin treatment on cell migration at 0 h and 24 h, with statistical analysis of wound closure percentage. (**F**) Transwell migration assay showing the impact of METTL5 overexpression and Scutellarin treatment on cell migration at 24 h, with quantification of migrated cell numbers. (**G**) Molecular docking illustration of METTL5 and Scutellarin.

Scutellarin-mediated suppression of malignant phenotypes, rescue experiments were performed in METTL5-overexpressing SKOV3 cells treated with Scutellarin. Both wound healing and transwell assays showed that METTL5 overexpression attenuated the inhibitory effects of Scutellarin on cell migration (Fig. 5E,F), suggesting that METTL5 plays a key role in mediating the anti-migratory activity of Scutellarin.

### METTL5 as a potential oncogenic factor in ovarian cancer

Using the GEPIA database, which integrates TCGA and GTEx datasets, we performed a pan-cancer analysis of METTL5 expression. The scatter plot revealed that METTL5 is highly expressed in samples from multiple cancer types, including ovarian cancer (Fig. 6A), which is consistent with findings reported in studies of other malignancies[9]. This suggests that METTL5 may be an important pan-cancer driver. A complementary pan-cancer analysis based on the multi-database TNMplot platform comparing 22 tumor/normal tissue pairs showed that METTL5 expression was higher in tumor samples across 21 pairs, with ovarian cancer showing the most pronounced increase (Fig. 6C). This aligns with the paired ovarian cancer analysis from the GEPIA database (Fig. 6A,D). Furthermore, we investigated the immunohistochemical staining results of METTL5 in 3 normal ovarian tissue samples and 11 ovarian cancer tissue samples from The Human Protein Atlas (HPA) database. In normal ovarian tissue, METTL5 protein expression was not detected in stromal cells. However, in all ovarian cancer samples, 7 out of 11 displayed varying degrees of cytoplasmic and membranous staining. Specifically, 3 samples showed 25-75% staining, and 3 samples showed greater than 75% staining (Fig. 6B). Survival analysis revealed that high expression of METTL5 was associated with worse overall survival (OS) and progression-free survival (PFS), while no significant difference was observed in post-progression survival (PPS) (Fig. 6E).

To further evaluate the prognostic value of METTL5 in ovarian cancer, we performed univariate and multivariate Cox regression analyses using TCGA's ovarian cancer dataset. In the univariate analysis, high METTL5 expression showed a trend towards poor prognosis (HR = 1.54, 95% CI 0.94–2.55, $P = 0.09$). After adjusting for clinical variables such as age, tumor stage, and tumor grade, the multivariate analysis indicated that high METTL5 expression remained a significant predictor of unfavorable overall survival (HR = 1.85, 95% CI 1.10–3.10, $P = 0.02$). These results suggest that METTL5 may serve as an independent prognostic factor for poor outcomes in ovarian cancer (Table 1).

Finally, using TCGA ovarian cancer data, We performed differential gene analysis between METTL5-high and METTL5-low groups. KEGG and GO enrichment analysis of the differentially expressed genes revealed that upregulated genes were enriched in pathways including "ribosome" and "cytoplasmic translation"[19], suggesting potential mechanisms through which METTL5 may promote tumorigenesis (Fig. 6F,G). The above findings suggest that METTL5 may be involved in the initiation and progression of ovarian cancer. And its specific biological functions warrant further investigation.

## Discussion

Scutellarin, a compound derived from natural herbs, has been reported to inhibit proliferation, migration, and promote apoptosis in various cancers through multiple mechanisms. In gastric cancer, Scutellarin suppresses tumor growth by modulating the PTEN/PI3K signaling pathway[14]. Another study on gastric cancer in rat models demonstrated that Scutellarin not only reduced tumor incidence but also exhibited chemoprotective effects, alleviating chemotherapy-induced side effects[20]. In breast cancer, Scutellarin inhibits tumor stem cell growth both in vitro and in vivo, downregulating stemness markers such as CD44[6]. Scutellarin also possesses cardiovascular protective effects, preserving tumor-associated endothelial barrier function, which helps counteract metastasis in triple-negative breast cancer[21]. In small cell lung cancer, Scutellarin works synergistically with cisplatin to induce autophagy, overcoming drug resistance[4]. Due to its anti-inflammatory and antioxidant properties, Scutellarin has shown promising therapeutic effects in inflammatory diseases, such as colitis-associated colorectal cancer[22,23]. While Scutellarin's efficacy has been validated in various cancers, research on its role in ovarian cancer remains limited, existing studies suggest that the combination of Scutellarin with cisplatin holds significant potential in ovarian cancer treatment[7].

In our study, we systematically evaluated the anti-tumor effects of Scutellarin across a panel of epithelial ovarian cancer cell lines selected to represent distinct histological subtypes and to reflect the underlying heterogeneity of ovarian cancer. OVCAR3 and OVCAR8, both harboring TP53 mutations and DNA repair deficiencies, are widely accepted as representative models of high-grade serous ovarian cancer (HGSOC). A2780, which is TP53 wild-type, exhibits molecular features more consistent with endometrioid or undifferentiated subtypes. Although SKOV3 does not fully mirror the molecular characteristics of HGSOC, it is extensively used in ovarian cancer research owing to its high reproducibility and experimental tractability, and has also been shown to exhibit certain phenotypic similarities to clear cell carcinoma. Our results indicate that Scutellarin exhibits broad-spectrum anti-proliferative and anti-migratory effects across these different ovarian cancer subtypes. While the therapeutic efficacy of Scutellarin has been primarily assessed in cell lines and mouse models in other cancers, these studies often lack models that reflect the tumor heterogeneity seen in patients. To better mimic the patient response, we established organoid models representing two distinct ovarian cancer subtypes. Our findings show that Scutellarin effectively inhibits the growth of ovarian cancer organoids and promotes cell death, as evidenced by morphological observations and PI staining. To refine the understanding of the underlying mechanisms, incorporating pathway-specific apoptotic markers, such as cleaved caspase-3 or Annexin V, would provide further validation of the cell death process induced by Scutellarin. Our results provide preliminary preclinical evidence for Scutellarin's therapeutic potential and supports its further translation into clinical applications.

To evaluate the therapeutic potential of Scutellarin in ovarian cancer, we selected concentrations ranging from 10 to 50 μM for functional assays, guided by previous pharmacological studies and experimental feasibility. Although Scutellarin exhibits low oral bioavailability, with the parent compound reaching a Cmax of less

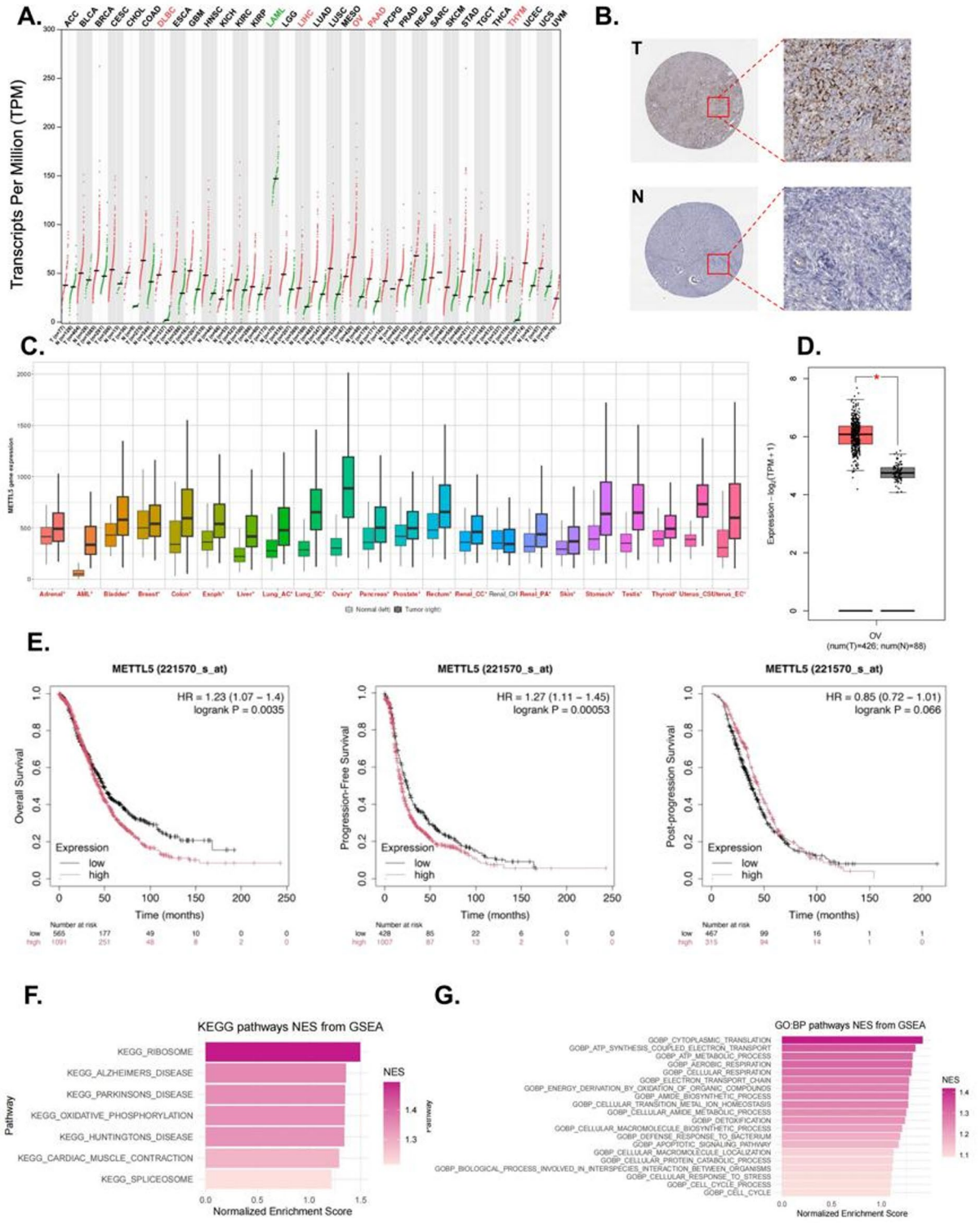


**Fig. 6**. Elevated METTL5 expression in ovarian cancer is associated with poorer clinical prognosis. (**A**) METTL5 mRNA expression in tumor and normal tissues across pan-cancer data from the GEPIA database, based on TCGA and GTEx, presented as TPM values. (**B**) Immunohistochemical staining of METTL5 in normal ovarian tissue and ovarian cancer samples from the HPA database, using antibody HPA038223, with images and magnified views. (**C**) METTL5 gene expression in 22 paired normal and tumor tissues, $^{*}P < 0.05$. (**D**) METTL5 expression in ovarian cancer and normal samples from the GEPIA database, $^{*}P < 0.01$. (**E**) Kaplan–Meier analysis of METTL5 expression in ovarian cancer, showing OS, PFS, and PPS. F and G. KEGG (**F**) and GO (**G**) biological process pathway enrichment analysis of upregulated genes in METTL5-high ovarian cancer samples.

| Variables | Univariate HR (95% CI) | *P* value | Multivariate HR (95% CI) | *P* value |
|---|---|---|---|---|
| Age (>65 vs. ≤65) | 1.58 (1.17 to 2.15) | 0.003 | 1.66 (1.22 to 2.27) | 0.001 |
| Stage (III–IV vs. I–II) | 1.87 (0.88 to 3.98) | 0.11 | 1.62 (0.74 to 3.55) | 0.23 |
| Tumor grade (G3=G4 vs. G1–G2) | 1.48 (0.92 to 2.38) | 0.11 | 1.37 (0.84 to 2.25) | 0.21 |
| METTL5 (High vs. Low) | 1.54 (0.94 to 2.55) | 0.09 | 1.85 (1.10 to 3.10) | 0.02 |

**Table 1**. Univariate and multivariate Cox analysis of METTL5 expression and overall survival in ovarian cancer.

than 5 ng/mL (~0.01 μM) in human plasma. It is rapidly metabolized into its active glucuronide metabolite, isoscutellarin, which reaches a Cmax of approximately 87 ng/mL (~0.19 μM)[15,24]. Moreover, Scutellarein, the main metabolite, has shown anti-proliferative activity in ovarian cancer cells at 25 μM by targeting EZH2/FOXO1 signaling[25]. Therefore, the use of sub-$IC_{50}$ concentrations in our assays is not only experimentally appropriate but also clinically relevant. Rather than focusing solely on cytotoxicity, we aimed to determine whether Scutellarin could modulate malignant phenotypes at these physiologically relevant concentrations. While Scutellarin did not significantly reduce cell viability in OVCAR3 cells—likely reflecting low cytotoxicity—it significantly inhibited colony formation and transwell migration in all four ovarian cancer cell lines. These results suggest that Scutellarin exerts anti-tumor effects by impairing proliferative and migratory capacities, rather than directly inducing cell death.

METTL5 is an underexplored molecule in ovarian cancer. Analysis of TCGA ovarian cancer data indicates that METTL5 is highly expressed at both the mRNA and protein levels in ovarian cancer, and its expression is associated with shorter overall survival and progression-free survival, highlighting its potential as a prognostic biomarker and therapeutic target. To further validate its clinical significance, we performed univariate and multivariate Cox proportional hazards regression analyses. While high METTL5 expression showed a trend toward poor prognosis in univariate analysis, it did not reach statistical significance. This borderline result may reflect limited statistical power and warrants further validation in larger cohorts. Importantly, in multivariate analysis, after adjusting for age, tumor stage, and grade, METTL5 remained a significant independent predictor of poor overall survival.

We further investigated whether Scutellarin exerts its anti-tumor effects by modulating METTL5. Although treatment with 10–25 μM Scutellarin did not significantly reduce METTL5 protein levels, it markedly suppressed proliferation and migration, suggesting that its mechanism may involve interference with METTL5 functional activity or downstream signaling rather than expression downregulation alone. At 50 μM, METTL5 expression was decreased in cell lines, and overexpression of METTL5 partially rescued the inhibitory effect of Scutellarin, supporting a METTL5-dependent mechanism. Although METTL5 enzymatic activity was not directly measured, prior studies have established its catalytic role in 18 S rRNA methylation[10]. Our study aimed to explore METTL5's biological role in ovarian cancer progression rather than its catalytic mechanism. As a natural flavonoid, Scutellarin is known to exert pleiotropic biological effects, and its multi-target potential cannot be excluded. While these preliminary results are promising, further in-depth studies are required to clarify the mechanistic role of METTL5 and to evaluate the clinical efficacy and safety of Scutellarin.

## Data availability

Data is contained within the article.

Received: 8 January 2025; Accepted: 20 May 2025
Published online: 27 May 2025

## References

1. Webb, P. M. & Jordan, S. J. Global epidemiology of epithelial ovarian cancer. *Nat. Rev. Clin. Oncol.* **21** (5), 389–400. https://doi.org/10.1038/s41571-024-00881-3 (2024).
2. Zhang, Y. et al. Scutellarin alleviates cerebral ischemia/reperfusion by suppressing oxidative stress and inflammatory responses via MAPK/NF-κB pathways in rats. *Environ. Toxicol.* **37** (12), 2889–2896. https://doi.org/10.1002/tox.23645 (2022).
3. Deng, W. et al. Scutellarin inhibits human renal cancer cell proliferation and migration via upregulation of PTEN. *Biomed. Pharmacother.* **107**, 1505–1513. https://doi.org/10.1016/j.biopha.2018.08.127 (2018).
4. Sun, C. Y. et al. Scutellarin increases cisplatin-Induced apoptosis and autophagy to overcome cisplatin resistance in Non-small cell lung Cancer via ERK/p53 and c-met/AKT signaling pathways. *Front. Pharmacol.* **9**, 92. https://doi.org/10.3389/fphar.2018.00092 (2018).
5. Cui, Z. et al. Scutellarin activates IDH1 to exert antitumor effects in hepatocellular carcinoma progression. *Cell. Death Dis.* **15** (4), 1–17. https://doi.org/10.1038/s41419-024-06625-6 (2024).
6. Ma, H. et al. Scutellarin, a flavonoid compound from Scutellaria Barbata, suppresses growth of breast cancer stem cells in vitro and in tumor-bearing mice. *Phytomedicine* **128**, 155418. https://doi.org/10.1016/j.phymed.2024.155418 (2024).
7. Xie, Z., Guo, Z., Lei, J. & Yu, J. Scutellarin synergistically enhances cisplatin effect against ovarian cancer cells through enhancing the ability of cisplatin binding to DNA. *Eur. J. Pharmacol.* **844**, 9–16. https://doi.org/10.1016/j.ejphar.2018.11.040 (2019).
8. Bennett, M. R., Shepherd, S. A., Cronin, V. A. & Micklefield, J. Recent advances in methyltransferase biocatalysis. *Curr. Opin. Chem. Biol.* **37**, 97–106. https://doi.org/10.1016/j.cbpa.2017.01.020 (2017).
9. Xia, P. et al. METTL5 stabilizes c-Myc by facilitating USP5 translation to reprogram glucose metabolism and promote hepatocellular carcinoma progression. *Cancer Commun. (Lond).* **43** (3), 338–364. https://doi.org/10.1002/cac2.12403 (2023).
10. Rong, B. et al. Ribosome 18S m6A methyltransferase METTL5 promotes translation initiation and breast Cancer cell growth. *Cell. Rep.* **33** (12), 108544. https://doi.org/10.1016/j.celrep.2020.108544 (2020).

11. Li, X., Yang, G., Ma, L., Tang, B. & Tao, T. N6-methyladenosine (m6A) writer METTL5 represses the ferroptosis and antitumor immunity of gastric cancer. *Cell. Death Discov.* **10** (1), 1–12. https://doi.org/10.1038/s41420-024-02166-1 (2024).
12. Bartha, Á. & Győrffy, B. TNMplot.com: A web tool for the comparison of gene expression in normal, tumor and metastatic tissues. *Int. J. Mol. Sci.* **22** (5), 2622. https://doi.org/10.3390/ijms22052622 (2021).
13. Győrffy, B. Integrated analysis of public datasets for the discovery and validation of survival-associated genes in solid tumors. *Innov. (Camb.)*. **5** (3), 100625. https://doi.org/10.1016/j.xinn.2024.100625 (2024).
14. Wang, Z. et al. Scutellarin suppressed proliferation and induced apoptosis in gastric cancer via Wnt/β-catenin signaling pathway. *Curr. Pharm. Des.* **29** (5), 368–378. https://doi.org/10.2174/1381612829666230130141931 (2023).
15. Li, M. et al. Scutellarin alleviates ovalbumin-induced airway remodeling in mice and TGF-β-induced pro-fibrotic phenotype in human bronchial epithelial cells via MAPK and Smad2/3 signaling pathways. *Inflammation*. **47** (3), 853–873. https://doi.org/10.1007/s10753-023-01947-7 (2024).
16. Sato, T. et al. Paneth cells constitute the niche for Lgr5 stem cells in intestinal crypts. *Nature*. **469** (7330), 415–418. https://doi.org/10.1038/nature09637 (2011).
17. Dutta, D., Heo, I. & Clevers, H. Disease modeling in stem cell-derived 3D organoid systems. *Trends Mol. Med.* **23** (5), 393–410. https://doi.org/10.1016/j.molmed.2017.02.007 (2017).
18. Kopper, O. et al. An organoid platform for ovarian cancer captures intra- and interpatient heterogeneity. *Nat. Med.* **25** (5), 838–849. https://doi.org/10.1038/s41591-019-0422-6 (2019).
19. Kanehisa, M. et al. KEGG: biological systems database as a model of the real world. *Nucleic Acids Res.* **53** (D1), D672–D677. https://doi.org/10.1093/nar/gkae909 (2025).
20. Sun, J. & Meng, M. Chemoprotective effect of scutellarin against gastric cancer in rats: an in vitro and in vivo study. *J. Oleo Sci.* **71** (7), 1003–1012. https://doi.org/10.5650/jos.ess21399 (2022).
21. Mei, X., Zhang, J. & Jia, W. nan, ya, et al. Scutellarin suppresses triple-negative breast cancer metastasis by inhibiting TNFα-induced vascular endothelial barrier breakdown. *Acta Pharmacol. Sin.* **43**(10), 2666–2677. https://doi.org/10.1038/s41401-022-00873-y (2022).
22. Zeng, S. et al. Scutellarin ameliorates colitis-associated colorectal cancer by suppressing Wnt/β-catenin signaling cascade. *Eur. J. Pharmacol.* **906**, 174253. https://doi.org/10.1016/j.ejphar.2021.174253 (2021).
23. Zeng, S. et al. Suppression of colitis-associated colorectal cancer by scutellarin through inhibiting Hedgehog signaling pathway activity. *Phytomedicine*. **98**, 153972. https://doi.org/10.1016/j.phymed.2022.153972 (2022).
24. Wang, L. & Ma, Q. Clinical benefits and pharmacology of scutellarin: a comprehensive review. *Pharmacol. Ther.* **190**, 105–127. https://doi.org/10.1016/j.pharmthera.2018.05.006 (2018).
25. Lang, X. et al. Scutellarein induces apoptosis and inhibits proliferation, migration, and invasion in ovarian cancer via Inhibition of EZH2/FOXO1 signaling. *J. Biochem. Mol. Toxic.* **35** (10), e22870. https://doi.org/10.1002/jbt.22870 (2021).


## Author contributions

Conceptualization, L.D., C.L.; methodology and software, L.D., C.L.; validation, C.L.; formal analysis and investigation, L.D., N.W., D.R.; resources and data curation, C.L.; writing-original draft preparation, L.D., C.L.; writing-review & editing, L.D., N.W.; visualization, W.C., Y.L.; supervision, Y.W., H.L.; project administration, Y.W., H.L.; funding acquisition, Y.W., H.L. All authors have read and agreed to the published version of the manuscript.

## Funding

This work was funded by the Natural Science Foundation of China (82174135, 82374163, 82172918, 82471723), Pudong New Area High Peak Plateau Traditional Chinese Medicine Hepatology Specialty Discipline (YC-2023-0610), Shanghai Public Health Excellent Discipline Leadership Program (GWVI-11.2-XD15).

## Declarations

## Competing interests

The authors declare no competing interests.

## Institutional review board statement

This study was conducted in accordance with the guidelines of the Helsinki Declaration and approved by the Ethics Committee of Renji Hospital (KY2021-244-B).

## Informed consent

Informed consent was obtained from the patients for the collection of tumor tissues.

## Additional information

**Supplementary Information** The online version contains supplementary material available at https://doi.org/10.1038/s41598-025-03411-y.

**Correspondence** and requests for materials should be addressed to Y.W. or H.L.